molecules

MDPI

Article

Reusable Magnetic Nanoparticle Immobilized Nitrogen-Containing Ligand for Classified and Easy Recovery of Heavy Metal Ions

Jingyun Jing and Congling Shi *

Beijing Key Laboratory of Metro Fire and Passenger Transportation Safety, China Academy of Safety Science and Technology, Beijing 100012, China; jingjingyun14@iccas.ac.cn

* Correspondence: shicl@chinasafety.ac.cn; Tel.: +86-010-8491-1844; Fax: +86-010-8973-1973

Academic Editors: Francesco Pellegrino, Federico Cesano, Marco Fabbiani and Chiara Negri
Received: 19 June 2020; Accepted: 9 July 2020; Published: 14 July 2020

Abstract: Functionalized Tris[2-(dimethylamino) ethyl] amine (Me_6TREN) ligands tethered-Fe_3O_4@Me_6TREN nanoparticles (NPs) with a size of 150 nm were prepared to achieve classified and easy recovery of heavy metal ions in wastewater. The preparation of such NPs related to sequential silane ligand exchange and a following cure and Schiff base reactions for Fe_3O_4 NPs. Fe_3O_4@Me_6TREN NPs as an effective nano-adsorbent of heavy metals exhibited significant differences in maximum adsorption capacity for Cr(III) (61.4 mg/g), Cu(II) (245.0 mg/g), Pb(II) (5.3 mg/g), and Cd(II) (1136.2 mg/g), in favor of classified removal of heavy metals from wastewater. Furthermore, Fe_3O_4@Me_6TREN NPs can be regenerated by desorbing metal ions from NP surfaces eluted with ethylenediaminetetraacetic acid disodium salt (EDTA-Na_2) aqueous, which endows such NPs promising potency as new nano-vectors for the removal of heavy metals.

Keywords: magnetic nanoparticle; surface modification; adsorption; heavy metal ions; regeneration

1. Introduction

Increasingly severe water pollution caused by heavy metals has posed a serious threat to human health [1], which is in a situation of urgent need to be handled worldwide [2–4]. Electroplating wastewater as the main pollution source is hazardous to the human body with a variety of heavy metal ions exceeding the standard [5–7]. The maximal permissible limit of Cr(III), Cu(II), Pb(II), and Cd(II) ions in drinking water is 0.05 mg/L, 2 mg/L, 0.01 mg/L, and 0.003 mg/L, respectively based on the World Health Organization [8].

Various efforts, such as chemical precipitation [9,10], ion exchange [11,12], membrane filtration [13,14], and adsorption [15,16] have been taken to remove heavy metal ions from wastewater. Among them, the adsorption method with activated carbon [17,18], carbon nanotube [19], sewage sludge ash [20], chitosan [21,22], and hydrogel [23] as adsorbents has been recognized as the most promising candidate for removal of heavy metals from polluted water [24,25] with superiority in cost and efficiency. Further, magnetic composite nanoparticles which can be removed conveniently from water with the help of an external magnet because of their exceptional properties possess better performance in removing heavy metal ions from water [26,27]. However, selective recovery of metal ions from water are challenging, which limits wide application of this method. Therefore, the development of new magnetic nano-adsorbents [28] with simplicity, effectiveness, and recyclability has great significance in classified recovery of heavy metal ions in wastewater.

Here, we aim to propose a facile approach to graft Me_6TREN ligands onto the surface of SiO_2-coated Fe_3O_4 to prepare functionalized Fe_3O_4@Me_6TREN nanoparticles (NPs) to act as a new nano-adsorbent of heavy metals in polluted water. As shown in Scheme 1, based on magnetic

polyethylene glycol (PEG)-capped Fe_3O_4 NPs synthesized via solvothermal method, silane ligand exchange and a following cure, Schiff base reactions and reduction by $NaBH_4$ were sequentially performed to make Me_6TREN-alike ligands tethered onto such NPs. Fe_3O_4@Me_6TREN NPs as a powerful nano-gripper can selectively concentrate some heavy metals to realize classified and easy recovery. Furthermore, the NPs can be regenerated by washing with stronger chelators of heavy metal ions, such as ethylenediaminetetraacetic acid disodium salt (EDTA-Na_2) aqueous. Such NPs with magnetic responsiveness and recyclability are a competitive medium for complexation of heavy metals.

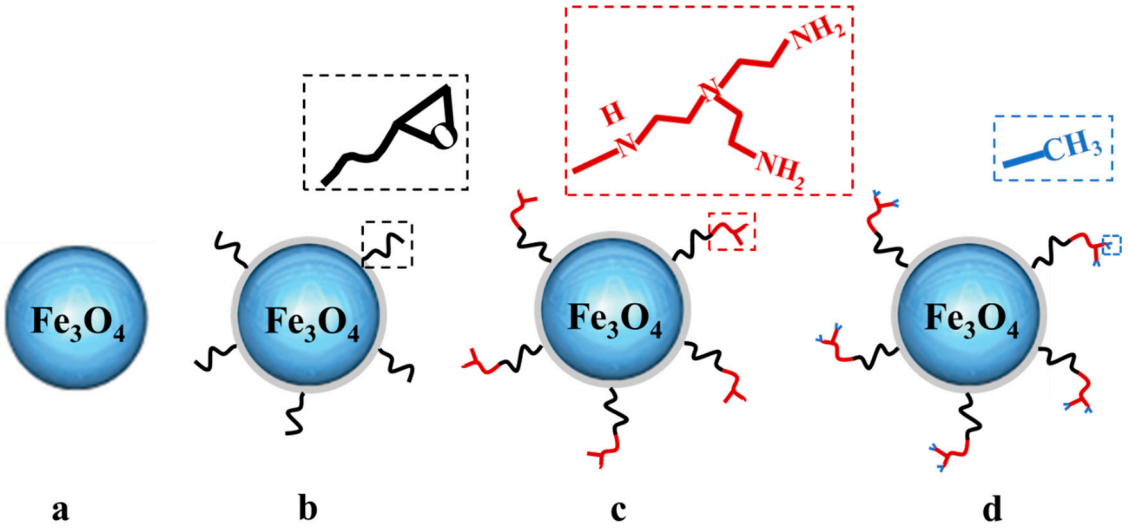

Scheme 1. Synthesis of Fe_3O_4@Me_6TREN nanoparticles (NPs): (**a**) Fe_3O_4 NP; (**b**) Fe_3O_4@epoxide NP; (**c**) Fe_3O_4@TAEA NP; (**d**) Fe_3O_4@Me_6TREA NP.

2. Results and Discussion

2.1. The Fe_3O_4@epoxide NPs

The Fe_3O_4 NPs were synthesized by the solvothermal method as reported previously [29]. The crystalline structure of the obtained NPs was confirmed by the XRD spectrum (Figure S1). The Fe_3O_4 NPs are ferromagnetic with a saturation magnetization of 73.7 emu/g and coercivity at 86 Oe (Figure 1a). The NPs were well-dispersed in ethanol with an approximate diameter of 150 nm (Figure 1b). The epoxide groups were then introduced onto the NP surface by sol-gel coating of an epoxide-functional silane KH560 [30]. The unmodified NPs show an absorption peak at 1462 cm^{-1}, which is assigned to the -CH_2- group of PEG. The strong IR band at 585 cm^{-1} is characteristic of the Fe-O vibrations related to the ferrite core. After KH560 treatment, the IR spectrum of the NPs displayed a strong absorption peak at 1100 cm^{-1}, which is characteristic of the Si-O-Si vibrations, indicating the formation of a silane layer on the NP surface. A peak at 915 cm^{-1} is evidence of the presence of epoxide group [31] (Figure 1c). Meanwhile, the modified NPs retain their original spherical shape and size as shown in the SEM image (Figure 1d).

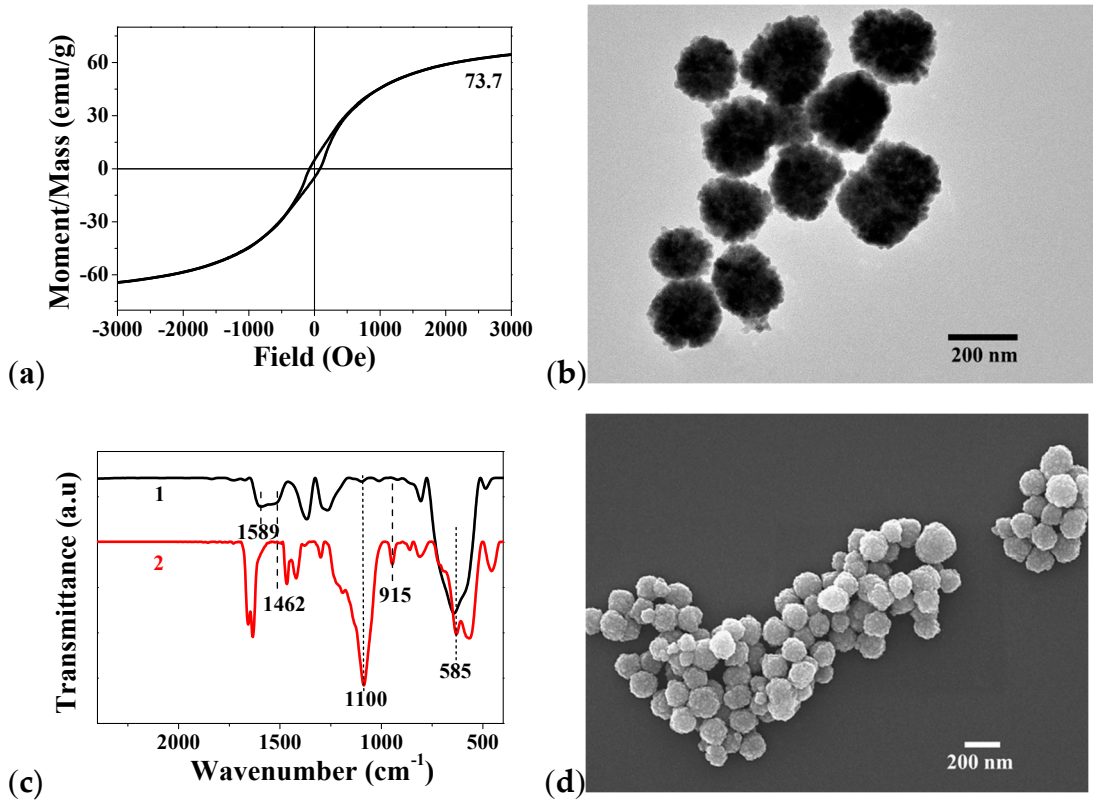

Figure 1. (**a**) VSM curve of the Fe_3O_4 NP; (**b**) TEM image of Fe_3O_4 NP; (**c**) Fourier transform infrared (FT-IR) spectra of Fe_3O_4 NP (1) and Fe_3O_4@epoxide NP (2); (**d**) SEM image of Fe_3O_4@epoxide NP.

2.2. The Fe_3O_4@Me_6TREN NP

The Fe_3O_4@TAEA NPs were synthesized by cure reaction of amino and epoxide groups with treatment of excessive TAEA against Fe_3O_4@epoxide NPs. To avoid crosslinking, 10-fold excess of TAEA was added, so only one out of three amino groups reacted with the epoxide. With the amino groups facing outward, zeta potential of the NPs dispersed in ethanol undergoes an obvious transformation from –13.8 mV (Figure 2a, curve 1) to 4.8 mV (Figure 2a, curve 2) after TAEA grafting. The two unreacted amino groups per TAEA unit were further reacted with formaldehyde under acidic conditions to form a Schiff base, and then reduced by $NaBH_4$. When all the primary amine groups were converted to tertiary amine, the Fe_3O_4@Me_6TREN NPs dispersed in ethanol holding a zeta potential of –3.4 mV (Figure 2a, curve 3) and a diameter of 142 nm (Figure 2b, curve 3) were obtained. In the IR spectra, the peaks assigned to -NH_2 group in primary amine between 3200–3450, 1533 and 1630 cm^{-1} completely disappeared after formation of tertiary amine (Figure 2c), which is evidence of successful surface modification. TGA measurements were performed to estimate the exact content of Me_6TREN ligands on the NP surface. The weight loss of the Fe_3O_4@Me_6TREN NPs increased by 0.19% compared to that of Fe_3O_4@epoxide NPs after heating to 700 °C, indicating that the NPs contain 0.20 wt% of Me_6TREN functionalities (Figure 2d).

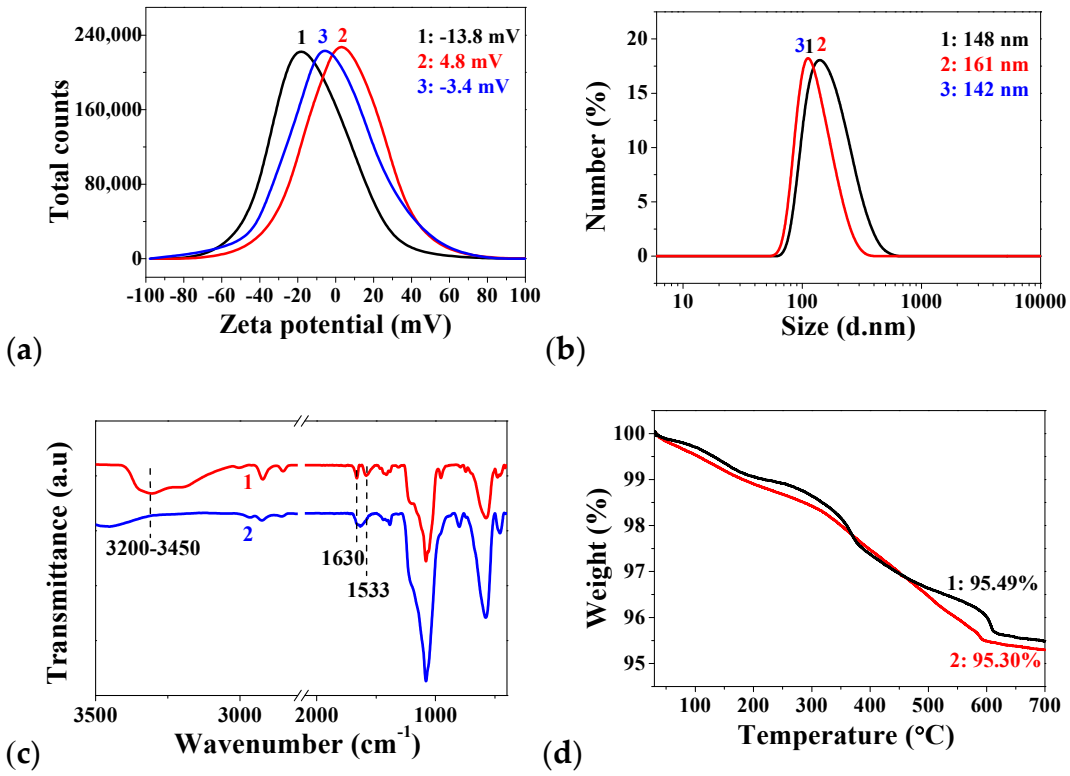

Figure 2. (**a**) Zeta potential and (**b**) DLS traces of Fe_3O_4@epoxide NP (1), Fe_3O_4@TAEA NP (2), and Fe_3O_4@Me_6TREN NP (3); (**c**) FT-IR spectra of Fe_3O_4@TAEA NP (1) and Fe_3O_4@Me_6TREN NP (2); (**d**) thermogravimetric analysis (TGA) curves of Fe_3O_4@epoxide NP (1) and Fe_3O_4@ Me_6TREN NP (2).

2.3. Adsorption of Heavy Metal Ions in Water with Fe_3O_4@Me_6TREN NPs

The Fe_3O_4@Me_6TREN NPs can serve as nano-grippers of heavy metal ions by complexation to achieve removal of metal ions from water. The zeta potential of aqueous solution of Fe_3O_4@Me_6TREN NPs undergoes a positive-to-negative transformation with the increase of pH value in the range from 3 to 7 and the isoelectric point falls around 6.1 measured on Nano ZS (Figure 3a), which has an influence on the adsorption performance for metal ions. The effect of pH value on adsorption capacity for four heavy metal ions (Cr(III), Cu(II), Pb(II), and Cd(II)) was studied by a UV–Vis spectrophotometer with an initial concentration of ~5 mg/mL for each metal salt compound. Standard curves of UV–Vis adsorption of four metal ions in water were measured beforehand (Figures S2–S5). Saturated adsorption capacity for metal ions can be calculated based on the Formula (1)

$$q_e = \frac{(C_0 - C_e) \times V}{m} \quad (1)$$

where q_e is equilibrium adsorption capacity; C_0 and C_e refer to the initial and equilibrium concentrations of metal ions in solution, respectively; V is the volume of solution; m stands for the mass of adsorbent. As shown in Figure 3b, the adsorption capacity of all four metal ions by Fe_3O_4@Me_6TREN NPs increases in the solution pH value window of 3–7 for weaker electrostatic repulsion between NP surfaces and metal ions in a higher pH value. However, the adsorption capacity of the NPs for four metal ions exhibits a great difference, which is the strongest for Cr(III) (61.4 mg/g), Cu(II) (245.0 mg/g), and Cd(II) (1136.2 mg/g), and the weakest for the Pb(II) ion (5.3 mg/g). The significant difference of adsorption capacity of the Fe_3O_4@Me_6TREN NPs for the selected four metal ions is beneficial for the classified recovery of heavy metal ions in wastewater.

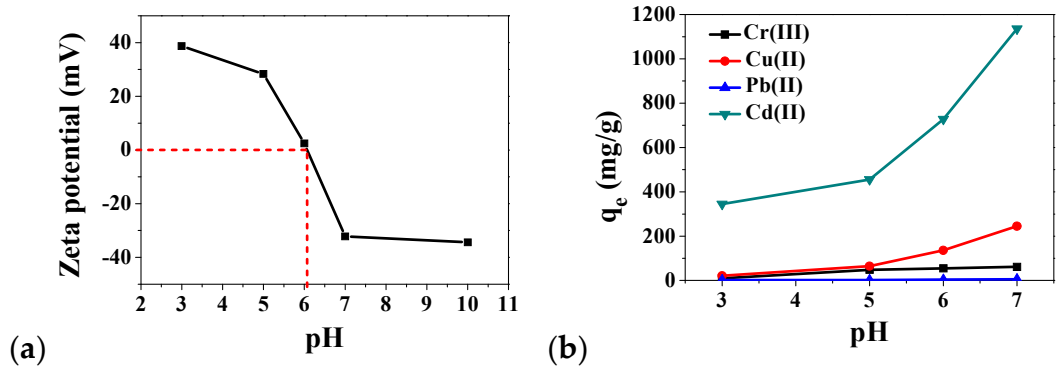

Figure 3. (**a**) Zeta potential of Fe_3O_4@Me_6TREN NPs aqueous dispersion at various pH values; (**b**) the effect of pH on adsorption capacity for four metal ions by Fe_3O_4@Me_6TREN NPs.

Similar batch experiments were performed to determine the effect of contact time on adsorption capacity. As Figure 4a–d illustrates, although adsorption capacity of Fe_3O_4@Me_6TREN NPs for four metal ions shows a dramatic difference, the dynamic adsorption process experiences a similar trend in a rapid growth in the early stage (50 min), followed by a gradual equilibrium process after approximately 120 min. Furthermore, to reveal the adsorption behavior of the NPs for Cr(III), Cu(II), Pb(II), and Cd(II) ions, adsorption kinetic data were fitted with two common models of pseudo-first-order Formula (2) and pseudo-second-order Formula (3) [32] (Figure 4a–d).

$$\text{Pseudo-first-order}: \ q = q_e\left(1 - e^{-k_1 t}\right) \tag{2}$$

$$\text{Pseudo-second-order}: \ q = \frac{{q_e}^2 k_2 t}{1 + q_e k_2 t} \tag{3}$$

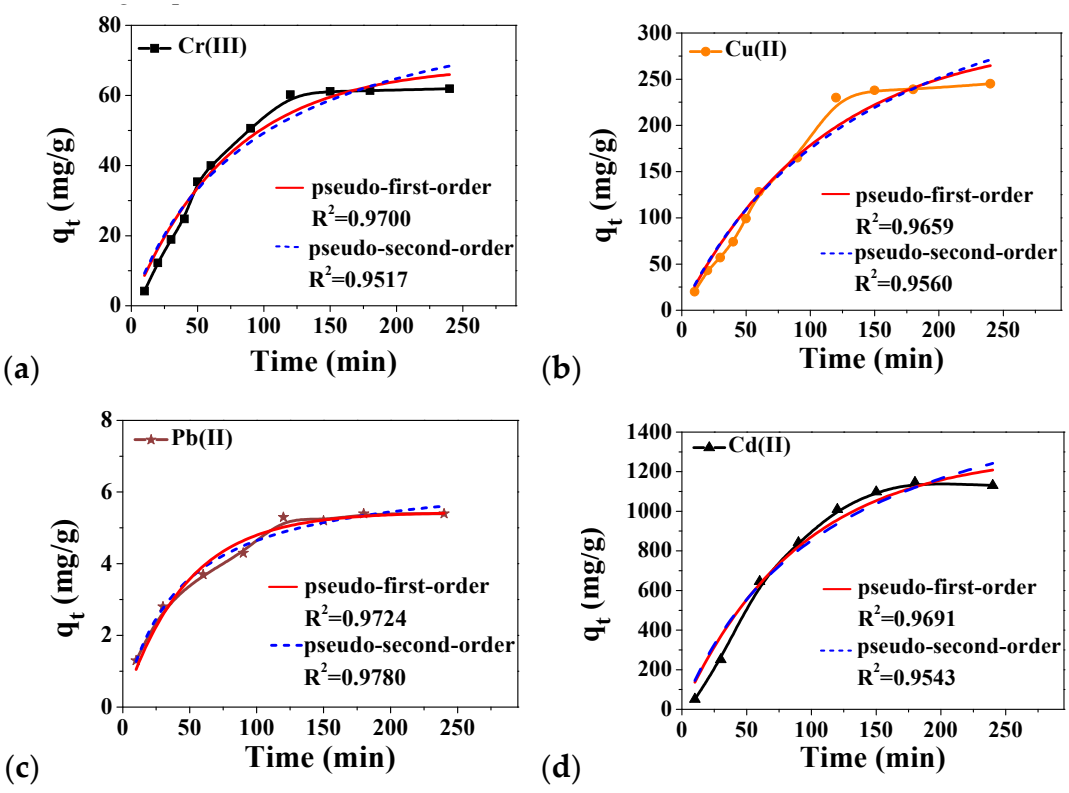

Figure 4. (**a**–**d**) Adsorption kinetic curves of four metal ions by Fe_3O_4@Me_6TREN NPs: (**a**) Cr(III); (**b**) Cu(II); (**c**) Pb(II); (**d**) Cd(II).

Details of kinetic parameters fitted with the two models are provided in Table 1. According to the results, the nonlinear fitting curve of the pseudo-first-order model presents a better correlation for Cr(III), Cu(II), and Cd(II) ions; the correlation coefficient R^2 values are all higher than 0.96, which is slightly larger than that of the pseudo-second-order model. The behavior of adsorption of Pb(II) ion supporting a pseudo-second order equation is in agreement with chemisorption being the rate controlling step [33].

Table 1. Adsorption kinetic parameters of the Fe_3O_4@Me_6TREN NPs for Cr(III), Cu(II), Pb(II), and Cd(II) ions.

Metal Ions	Pseudo-First-Order			Pseudo-Second-Order		
	q_e (mg·g^{-1})	k_1 (min^{-1})	R^2	q_e (mg·g^{-1})	k_2 (mg·g^{-1}·min^{-1})	R^2
Cr(III)	68.7	1.34×10^{-2}	0.9700	94.5	2.20×10^{-5}	0.9517
Cu(II)	298.0	0.91×10^{-2}	0.9659	446.2	1.47×10^{-5}	0.9556
Pb(II)	5.4	2.14×10^{-2}	0.9724	6.6	3.60×10^{-3}	0.9780
Cd(II)	1298.0	1.11×10^{-2}	0.9691	1842.8	4.67×10^{-6}	0.9543

The adsorption isotherms of magnetic NPs for Cr(III), Cu(II), and Cd(II) ions are presented in Figure 5. The Langmuir and Freundlich models were used to simulate the adsorption isotherms, which can be represented in the following Equations (4) and (5):

$$\text{Langmuir isotherm}: \frac{C_e}{q_e} = \frac{C_e}{q_m} + \frac{1}{K_L q_m} \quad (4)$$

$$\text{Freundlich isotherm}: lgq_e = lgK_F + \frac{1}{n} lgC_e \quad (5)$$

where C_e (mg/L) is the equilibrium concentration of metal ions in solution; q_e (mg/g) and q_m (mg/g) are the equilibrium and maximum adsorption capacity, respectively; K_L (L/mg) is the constant of Langmuir isotherm; K_F and n are the constants of the Freundlich isotherm.

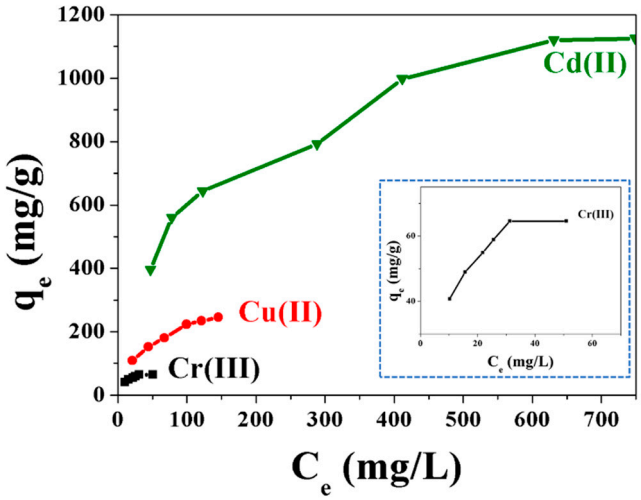

Figure 5. Adsorption isotherms of Fe_3O_4@Me_6TREN NPs for Cr(III), Cu(II), and Cb(II) ions.

The parameters related to the Langmuir and Freundlich isotherm models were given in Table 2. According to the results, the Langmuir model represents a little more goodness-of-fit than the Freundlich model for three metal ions based on the correlation coefficient (R^2). Furthermore, 1/n as the heterogeneity factor to describe the favoring degree of adsorption process was less than 0.5, suggesting superbly favorable adsorption for the three metal ions.

Table 2. Adsorption isotherm parameters for the removal of Cr(III), Cu(II), and Cd(II) ions by the Fe_3O_4@Me_6TREN NPs.

Metal Ions	Langmuir			Freundlich		
	q_m(mg/g)	K_L (L/g)	R^2	K_F	1/n	R^2
Cr(III)	76.6	0.122	0.989	15.85	0.404	0.987
Cu(II)	323.6	0.023	0.990	33.11	0.411	0.983
Cd(II)	1312.3	0.008	0.987	100.00	0.376	0.975

2.4. Desorption of Heavy Metal Ions from Fe_3O_4@Me_6TREN NPs

The Fe_3O_4@Me_6TREN NPs can be regenerated by desorbing metal ions from NP surfaces with EDTA-Na_2 (1:1 to the mol of metal ions) as a stronger chelator. To study the desorption efficiency, a comparison between adsorption mass (m_1) and desorption mass (m_2) per mg of NPs for each metal ion was analyzed using the concentration of the residual metal ion in solution after adsorption (C_1) and that after desorption (C_2) measured by ICP-MS. As shown in Table 3, EDTA-Na_2 exhibited excellent adsorption capacity for these metal ions, thus causing a desorption efficiency higher than 95% for metal ions except the Pb(II) ion from NPs. Furthermore, there was no significant difference in the shape and size of Fe_3O_4@Me_6TREN NPs after recycling, observed in SEM (Figure S6), and the element composition of NPs before and after desorption were characterized by SEM-EDX (Figure S6). In addition, NPs possessed a steady adsorption capacity for metal ions after three cycles (Figure 6c), meaning that such NPs are of great potentiality for reuse.

Table 3. Inductively coupled plasma mass spectrometry (ICP-MS) results of adsorption and desorption of various heavy metal ions.

Metal Ions	Adsorption		Desorption	
	C_1 (ng/g)	m_1 (mg)	C_2 (ng/g)	m_2 (mg)
Cr(III)	157.52	0.059	44.60	0.061
Cu(II)	208.51	0.254	127.56	0.242
Pb(II)	775.97	0.004	6.29	0.003
Cd(II)	236.23	1.003	435.71	0.956

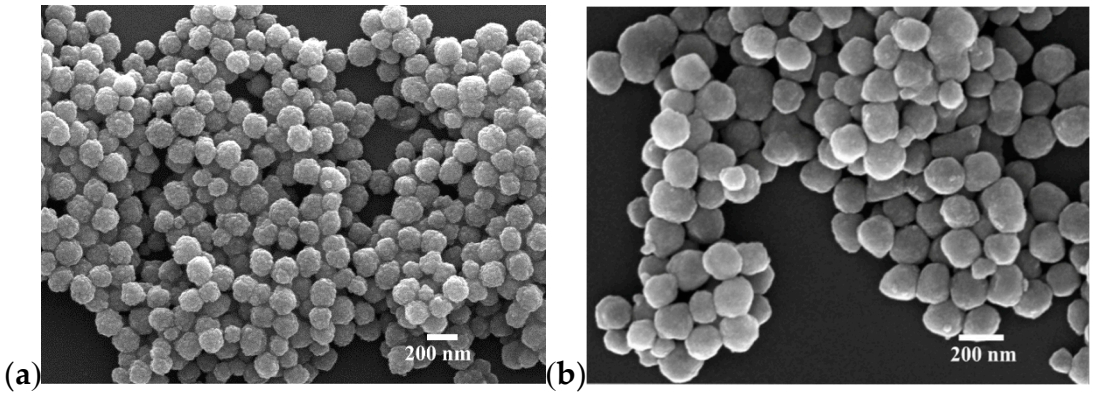

Figure 6. *Cont.*

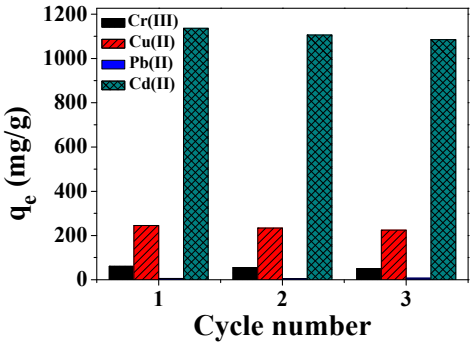

Figure 6. SEM images of Fe_3O_4@Me_6TREN NPs after (**a**) adsorption and (**b**) desorption of heavy metal ions, respectively; (**c**) adsorption capacity of NPs after recycling three times.

3. Materials and Methods

3.1. Materials

Ferric chloride hexahydrate ($FeCl_3 \cdot 6H_2O$), ethylene glycol, ethylenediaminetetraacetic acid disodium salt (EDTA-Na_2), formaldehyde solution (38% in water), sodium acetate, anhydrous cupric sulfate ($CuSO_4$), lead denitrate ($Pb(NO_3)_2$), cadmium nitrate ($Cd(NO_3)_2$), and chromic chloride hexahydrate ($CrCl_3 \cdot 6H_2O$) were purchased from Sinopharm Chemical Reagent. 3-Glycidoxypropyltrimethoxy silane (KH560) and tris(2-aminoethyl) amine (99%) were purchased from J&K Scientific. Polyethylene glycol (PEG, Mn = 20 kg/mol) was purchased from Sigma Aldrich. Sodium borohydride ($NaBH_4$) was purchased from Jinke Institute of Fine Chemicals. Acetic acid, hydrochloric acid, acetonitrile, ethylene glycol, and ethanol absolute (analytical reagent, AR) were purchased from Beijing Chemical Reagent. Toluene was purchased from XiLong Scientific. All reagents were used as received unless specified.

3.2. Synthesis of PEG-Capped Fe_3O_4 NPs

$FeCl_3 \cdot 6H_2O$ (2.36 g, 8.74 mmol), PEG (1.75 g, 8.75×10^{-2} mmol), and sodium acetate (3.14 g, 38 mmol) were dissolved in 70 mL of ethylene glycol under sonication. The yellow viscous liquid was then transferred into a sealed stainless steel autoclave with PTFE lining and heated at 180 °C for 8 h. After the autoclave was cooled down, the product NP was collected with a laboratory neodymium magnet, washed with water and ethanol three times, and stored in ethanol to avoid aggregation.

3.3. Synthesis of Epoxide-Capped Fe_3O_4 NPs (Fe_3O_4@epoxide)

PEG-capped Fe_3O_4 NPs were pre-treated by sonication in 0.1 M HCl for 10 min to generate more hydroxyl groups on the NP surface. A dispersion was prepared by adding 0.30 g of pre-treated Fe_3O_4 NPs into 100 mL of ethanol containing 3.0 µL of acetic acid. Then, 0.10 g (0.42 mmol) KH560 was added dropwise, and the mixture was stirred for 12 h at room temperature. The Fe_3O_4@epoxide NPs were washed with ethanol, collected with a magnet, and redispersed in ethanol for storage.

3.4. Synthesis of Tris(2-aminoethyl) Amine-Grafted Fe_3O_4 NPs (Fe_3O_4@TAEA)

To a dispersion of 0.1 g Fe_3O_4@epoxide NPs in 50 mL ethanol, 6.3 mL (10-fold excessive of theoretical epoxide content) of tris(2-aminoethyl) amine were added. The reaction mixture was stirred for 12 h at 60 °C to ensure a full reaction between the epoxy and amino groups. The obtained Fe_3O_4@TAEA NPs were then collected with a magnet, washed, and redispersed in ethanol.

3.5. Synthesis of Me_6TREN-Grafted Fe_3O_4 NP Ligand (Fe_3O_4@Me_6TREN)

To a dispersion containing 0.1 g Fe_3O_4@TAEA NPs and 60 µL of acetic acid in 50 mL acetonitrile, 0.5 mL of 38% formaldehyde solution was added. The reactants were stirred at room temperature for

2 h. Subsequently, the dispersion was cooled down to 0 °C, and a solution of 0.10 g $NaBH_4$ in 0.5 mL water was slowly added within 30 min via a syringe pump. Then the temperature was raised to 35 °C and kept for 24 h. The resulting Fe_3O_4@Me_6TREN NPs were washed with ethanol, collected with a magnet, and then dried in a vacuum oven.

3.6. Adsorption of Heavy Metal Ions in Water with Fe_3O_4@Me_6TREN NPs

Next, 2 mg of Fe_3O_4@Me_6TREN NPs were dispersed in 6 mL of Cr(III), Cu(II), Pb(II), and Cd(II) ions aqueous with an initial concentration (C_0) of 5 mg/mL for each metal salt compound and different pH value at 30 °C to investigate the effect of pH value on adsorption capacity. Similar experiments of adsorption kinetics were performed at C_0 = 5 mg/mL, pH = 7, and 30 °C. Adsorption isotherms were investigated with the initial concentration of metal ions ranging from 10 to 800 mg/L at pH = 7. The concentration of metal ions in water was measured by a UV–Vis spectrophotometer.

3.7. Desorption of Heavy Metal Ions from Fe_3O_4@Me_6TREN NPs

EDTA-Na_2 (same equiv. as metal ions) was dissolved into 3 mL aqueous dispersion containing Fe_3O_4@Me_6TREN/metal ion NPs at pH = 4. The mixture was stirred at 30 °C for 2 h. Fe_3O_4@Me_6TREN NPs were recycled by a magnet. The remaining supernatant was diluted with water and then determined by inductively coupled plasma mass spectrometry (ICP-MS) to detect the metal ions content.

3.8. Characterization

Transmission electron microscopy (TEM) measurements were performed on JEM-1011 at an accelerating voltage of 100 kV. Scanning electron microscopy (SEM) measurements were performed on Hitachi S-4800 at an accelerating voltage of 15 kV. Particle size distribution and zeta potential were measured on Nano ZS (Malvern Instruments). Crystallinity of the NPs was characterized by Rigaku D/max-2500. The magnetic property was measured using PPMS-9 (Quantum Design Inc., USA) at a magnetic field of 1 T. Fourier transform infrared (FT-IR) spectra were collected on a Bruker Equinox 55 spectrometer. Thermogravimetric analysis (TGA) was performed on PerkinElmer Pyris 1 in air at a heating rate of 10 °C/min. UV–Vis spectrophotometry was performed on TU-1901 to measure the concentration of four heavy metal ions in water. Inductively coupled plasma mass spectrometry (ICP-MS) measurement was performed on Thermo iCAP RQ to analyze the content of the metal ions.

4. Conclusions

Versatile and recyclable Fe_3O_4@Me_6TREN NPs as an efficient nano-adsorbent for the removal of heavy metal ions in wastewater were successfully prepared by a simple method in this work. The coating Me_6TREN is responsible for immobilization of heavy metal ions on NP surfaces with selective adsorption efficiency while the core Fe_3O_4 is in charge of magnetic responsiveness. Furthermore, Fe_3O_4@Me_6TREN NPs can be regenerated by desorbing heavy metal ions from NPs with EDTA-Na_2, which will be of great significance for cost reduction and further industrial application. It endows the Fe_3O_4@Me_6TREN NPs with the ability to be a powerful nano-catcher for classified recovery of heavy metal ions, which can be manipulated by the magnetic field.

Supplementary Materials: The following are available online, Additional XRD pattern, standard UV–Vis curves, and SEM-EDX images are included.

Author Contributions: Conceptualization, Methodology, Software, Validation, Formal Analysis, Investigation, Resources, Data Curation, Visualization, Writing-Original Draft Preparation, J.J. Supervision, Project Administration, Funding Acquisition, C.S. Writing-Review & Editing, C.S. and J.J. All authors have read and agreed to the published version of the manuscript.

Funding: This work was supported by the Fundamental Science Research Foundation of China Academy of Safety Science and Technology (grant numbers 2020JBKY02, 2020JBKY01) and the National High Level Talents Special Support Plan—"Ten Thousand Plan" (grant number WRJH201801).

Conflicts of Interest: The authors declare no conflict of interest.

References

1. Sharma, Y.C.; Srivastava, V.; Singh, V.K.; Kaul, S.N.; Weng, C.H. Nano-adsorbents for the removal of metallic pollutants from water and wastewater. *Environ. Technol.* **2009**, *30*, 583. [CrossRef] [PubMed]
2. Awual, M.R. Assessing of lead(III) capturing from contaminated wastewater using ligand doped conjugate adsorbent. *Chem. Eng. J.* **2016**, *289*, 65–73. [CrossRef]
3. Fu, F.L.; Wang, Q. Removal of heavy metal ions from wastewaters: A review. *J. Environ. Manag.* **2011**, *92*, 407–418. [CrossRef] [PubMed]
4. Carolin, C.F.; Kumar, P.S.; Saravanan, A.; Joshiba, G.J.; Naushad, M. Efficient techniques for the removal of toxic heavy metals from aquatic environment: A review. *J. Environ. Chem. Eng.* **2017**, *5*, 2782–2799. [CrossRef]
5. Cao, J.S.; Wang, C.; Fang, F.; Lin, J.X. Removal of heavy metal Cu(II) in simulated aquaculture wastewater by modified palygorskite. *Environ. Pollut.* **2016**, *219*, 924–931. [CrossRef]
6. Qu, J.H.; Tian, X.; Jiang, Z.; Cao, B.; Akindolie, M.S.; Hu, Q.; Feng, C.C.; Feng, Y.; Meng, X.L.; Zhang, Y. Multi-component adsorption of Pb(II), Cd(II) and Ni(II) onto microwave-functionalized cellulose: Kinetics, isotherms, thermodynamics, mechanisms and application for electroplating wastewater purification. *J. Hazard. Mater.* **2020**, *387*, 121718. [CrossRef]
7. Isaac, R.A.; Gil, L.; Cooperman, A.N.; Hulme, K.; Eddy, B.; Ruiz, M.; Jacobson, K.; Larson, C.; Pancorbo, O.C. Corrosion in drinking water distribution systems: A major contributor of copper and lead to wastewaters and effluents. *Environ. Sci. Technol.* **1997**, *31*, 3198–3203. [CrossRef]
8. *Guidelines for Drinking-Water Quality*, 4th ed.; World Health Organization: Geneva, Switzerland, 2011; pp. 398–403.
9. Chen, Q.Y.; Yao, Y.; Li, X.Y.; Lu, J.; Zhou, J.; Huang, Z.L. Comparison of heavy metal removals from aqueous solutions by chemical precipitation and characteristics of precipitates. *J. Water Process. Eng.* **2018**, *26*, 289–300. [CrossRef]
10. Chen, Q.Y.; Luo, Z.; Hills, C.; Xue, G.; Tyrer, M. Precipitation of heavy metals from wastewater using simulated flue gas: Sequent additions of fly ash, lime and carbon dioxide. *Water Res.* **2009**, *43*, 2605–2614. [CrossRef]
11. Matyjaszewski, K.; Pintauer, T.; Gaynor, S. Removal of copper-based catalyst in atom transfer radical polymerization using ion exchange resins. *Macromolecules* **2000**, *33*, 1476–1478. [CrossRef]
12. Beker, U.G.; Guner, F.S.; Dizman, M.; Erciyes, A.T. Heavy metal removal by ion exchanger based on hydroxyethyl cellulose. *J. Appl. Polym. Sci.* **1999**, *74*, 3501–3506. [CrossRef]
13. Sheng, D.; Liu, X.H.; Liao, J.B.; Lin, H.; Liu, F. PEI modified multiwalled carbon nanotube as a novel additive in PAN nanofiber membrane for enhanced removal of heavy metal ions. *Chem. Eng. J.* **2019**, *375*, 122086.
14. Zhao, F.Y.; Ji, Y.L.; Weng, X.D.; Mi, Y.F.; Ye, C.C.; An, Q.F.; Gao, C.J. High-flux positively charged nanocomposite nanofiltration membranes filled with poly(dopamine) modified multiwall carbon nanotubes. *ACS Appl. Mater. Inter.* **2016**, *8*, 6693–6700. [CrossRef] [PubMed]
15. Niu, Y.L.; Hu, W.; Guo, M.M.; Wang, Y.L.; Jia, J.P.; Hu, Z.B. Preparation of cotton-based fibrous adsorbents for the removal of heavy metal ions. *Carbohyd. Polym.* **2019**, *225*, 1152182. [CrossRef] [PubMed]
16. Lia, Y.Q.; Guo, C.F.; Shi, R.H.; Zhang, H.; Gong, L.Z.; Dai, L.B. Chitosan/ nanofibrillated cellulose aerogel with highly oriented microchannel structure for rapid removal of Pb(II) ions from aqueous solution. *Carbohyd. Polym.* **2019**, *223*, 115048. [CrossRef] [PubMed]
17. Li, H.; Zheng, F.; Wang, J.; Zhou, J.M.; Huang, X.H.; Chen, L.; Hu, P.F.; Gao, J.M.; Zhen, Q.; Bashir, S. Facile preparation of zeolite-activated carbon composite from coal gangue with enhanced adsorption performance. *Chem. Eng. J.* **2020**, *390*, 124513. [CrossRef]
18. Li, C.; Ma, H.Y.; Venkateswaran, S.; Hsiao, B.S. Highly efficient and sustainable carboxylated cellulose filters for removal of cationic dyes/heavy metals ions. *Chem. Eng. J.* **2020**, *389*, 123458. [CrossRef]
19. Salam, M.A. Removal of heavy metal ions from aqueous solutions with multi-walled carbon nanotubes: Kinetic and thermodynamic studies. *Int. J. Environ. Sci. Technol.* **2013**, *10*, 677–688. [CrossRef]
20. Militaru, B.A.; Pode, R.; Lupa, L.; Schmidt, W.; Tekle-Röttering, A.; Kazamer, N. Using sewage sludge ash as an efficient adsorbent for Pb(II) and Cu(II) in single and binary systems. *Molecules* **2020**, *25*, 2559. [CrossRef]

21. Liang, X.X.; Wang, N.; Qu, Y.L.; Yang, L.Y.; Wang, Y.G.; Ouyang, X.K. Facile preparation of metal-organic framework (MIL-125)/chitosan beads for adsorption of Pb(II) from aqueous solutions. *Molecules* **2018**, *23*, 1524. [CrossRef]
22. Zhuang, P.F.; Zhang, P.; Li, K.; Kumari, B.; Li, D.; Mei, X.F. Silver nanoclusters encapsulated into metal–organic frameworks for rapid removal of heavy metal ions from water. *Molecules* **2019**, *24*, 2442. [CrossRef] [PubMed]
23. Kulal, P.; Badalamoole, V. Magnetite nanoparticle embedded Pectin-graft-poly(N-hydroxyethylacrylamide) hydrogel: Evaluation as adsorbent for dyes and heavy metal ions from waste water. *Int. J. Biol. Macromol.* **2020**, *156*, 1408–1417. [CrossRef] [PubMed]
24. Ngambia, A.; Ifthikar, J.; Shahib, I.I.; Jawad, A.; Shahzad, A.; Zhao, M.M.; Wang, J.; Chen, Z.L.; Chen, Z.Q. Adsorptive purification of heavy metal contaminated wastewater with sewage sludge derived carbon-supported Mg(II) composite. *Sci. Total Environ.* **2019**, *691*, 306–321. [CrossRef] [PubMed]
25. Ma, J.C.; Fang, S.W.; Shi, P.; Duan, M. Hydrazine-functionalized guar-gum material capable of capturing heavy metal ions. *Carbohyd. Polym.* **2019**, *223*, 115137. [CrossRef] [PubMed]
26. Liu, X.W.; Hu, Q.Y.; Fang, Z.; Zhang, X.J.; Zhang, B.B. Magnetic chitosan nanocomposites: A useful recyclable tool for heavy metal ion removal. *Langmuir* **2009**, *25*, 3–8. [CrossRef] [PubMed]
27. Song, J.; Kong, H.; Jang, J. Adsorption of heavy metal ions from aqueous solution by polyrhodanine-encapsulated magnetic nanoparticles. *J. Colloid. Interf. Sci.* **2011**, *395*, 505–511. [CrossRef]
28. Ling, L.; Huang, X.Y.; Zhang, W.X. Enrichment of precious metals from wastewater with core-shell nanoparticles of iron. *Adv. Mater.* **2018**, *30*, e1705703. [CrossRef]
29. Huang, J.L.; Fan, L.Q.; Gu, Y.; Geng, C.L.; Luo, H.; Huang, Y.F.; Lin, J.M.; Wu, J.H. One-step solvothermal synthesis of high-capacity Fe_3O_4/reduced graphene oxide composite for use in Li-ion capacitor. *J. Alloy. Compd.* **2019**, *788*, 1119e1126. [CrossRef]
30. Weng, S.F.; Xu, Y.; Zhuang, Z. *Fourier Transform Infrared Spectroscopy*, 3rd ed.; Chemical Industry Press: Beijing, China, 2016.
31. De Palma, R.; Peeters, S.; Van Bael, M.J.; Van den Rul, H.; Bonroy, K.; Laureyn, W.; Mullens, J.; Borghs, G.; Maes, G. Silane ligand exchange to make hydrophobic superparamagnetic nanoparticles water-dispersible. *Chem. Mater.* **2007**, *19*, 1821–1831. [CrossRef]
32. Boamah, P.O.; Huang, Y.; Hua, M.Q.; Onumah, J.; Sam-Amoah, L.K.; Qian, Y.; Zhang, Q. Sorption of copper onto low molecular weight chitosan derivative from aqueous solution. *Ecotox. Environ. Safety* **2016**, *129*, 154–163. [CrossRef]
33. Ertugay, N.; Malkoc, E. Adsorption isotherm, kinetic, and thermodynamic studies for methylene blue from aqueous solution by needles of *Pinus sylvestris* L. *Pol. J. Environ. Stud.* **2014**, *23*, 1995–2006.

Sample Availability: Not available.